Carrier transport and light-spot movement in carbon-nanotube infrared emitters

Jing Guo[a)]
Department of Electrical and Computer Engineering, University of Florida, Gainesville, Florida 32611-6130

Muhammad A. Alam
School of Electrical and Computer Engineering, Purdue University, West Lafayette, Indiana 47907-1285

(Received 22 September 2004; accepted 9 November 2004; published online 3 January 2005)

Infrared emission from a carbon-nanotube (CNT) field-effect transistor, with the position of the light spot controlled by applied bias, was recently reported. In this letter, a self-consistent simulation, which couples a quantum treatment of the metal–CNT contacts to a semiclassical treatment of the channel, is performed to understand carrier transport and light emission in a CNT infrared emitter. The results show that when the channel is long, light emission significantly affects carrier transport, and reduces the source–drain current by a factor of 2 in ambipolar transport regime. The experimentally observed light-spot movement along the channel can be mostly understood and explained by a simple, semiclassical picture. © *2005 American Institute of Physics*.
[DOI: 10.1063/1.1848186]

Although application of carbon nanotubes (CNTs) in electronic devices has been extensively pursued in the last decade,[1,2] its application in optoelectronics has begun only recently. Since the first demonstration of light emission from an ambipolar CNT field-effect transistor (FET),[3] rapid advance in CNT optoelectronics has been achieved.[4–7] An interesting behavior of CNT IR emitters due to the one-dimensional channel geometry was recently reported.[7] Infrared emission[8] from a long CNT forms a light spot, which moves along the tube with applied bias. A detailed theoretical study of the experiment can provide important insights into how interplay of electrostatics, carrier transport, and optical radiation interplay determines both the electrical and optical properties of a long-channel CNTFET.

In this letter, a self-consistent simulation is performed for a long-channel CNTFET with IR emission. A quantum treatment of carrier tunneling through the metal–CNT contacts is coupled to a semiclassical treatment of carrier transport and infrared emission in the channel. The results show that carrier transport in the long channel is significantly affected by infrared emission at ambipolar-transport regime. Both electron current and hole current are strongly position-dependent near the light spot, and the total source–drain current is reduced by a factor up to 2. The major features of the light-spot movement observed in the experiment can be captured and understood using a simple, semiclassical picture. The simulation results indicate strong correlation between the optical and the electrical properties of a long-channel CNTFET.

In order to understand the experimental results for a CNT IR emitter reported by Freitag *et al.*,[7] a CNT emitter with a geometric size similar to the experiment is simulated. A coaxial gate rather than a planar gate is used to facilitate self-consistent simulation.[9] (The gate geometry is not central to the study, i.e., the conclusions about carrier transport and light-spot movement remain true for planar-gate geometry.) The gate oxide thickness is $t_{ox}=100$ nm, the contact radius is $r_c=30$ nm, the tube diameter is $d\approx 2$ nm, and the tube length is $L_{ch}=10$ μm. Because light emission occurs when the transistor is biased at ambipolar transport regime, a mid-gap metal-CNT Schottky barrier ($\Phi_{Bn}=\Phi_{Bp}=E_G/2$) is assumed in the simulation.

A self-consistent simulation between Poisson equation and the carrier transport equation is performed to simulate the CNT IR emitter. Figure 1 outlines the method for solving the transport equation. When the transistor is biased at ambipolar transport regime, holes are injected from the source to the channel and electrons are injected from the drain. The hole current through the Schottky barrier (SB) is computed using a quantum treatment,[10]

$$I_h = \frac{4q}{h}\int dET(E)[f_0(E-F_h) - f_0(E-E_{FS})], \tag{1}$$

where $T(E)$ is the transmission probability through the SB (computed by the Wentzel–Kramers–Brillouin approxima-

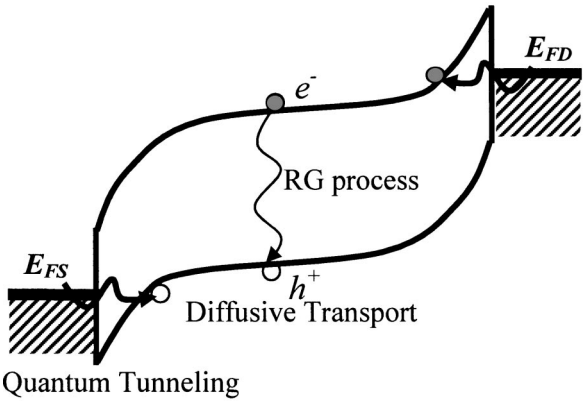

FIG. 1. Solving the transport equation for a long-channel CNTFET at ambipolar regime. A quantum treatment is used to compute the currents through the Schottky barriers at the ends of the channel. A semiclassical drift-diffusion treatment is used to describe carrier transport in the long channel, along with a band-to-band recombination process to describe infrared emission.

[a)]Electronic mail: guoj@ufl.edu

tion for tunneling and equal to 1 for thermionic emission), F_h is the hole quasi-Fermi level in the channel, E_{FS} is the source Fermi level, and f_0 is the Fermi–Dirac distribution function. The electron current injected from the drain is computed similarly.

The long channel length imposes challenges for a full quantum treatment, but carrier transport at this length scale is dominated by scattering and can be described by a drift-diffusion equation. (For example, $I-V$ characteristics of CNTFETs with a channel length down to about 1 μm can be described by the square law,[11,12] which is derived from a drift-diffusion treatment of the channel.[13]) Drift-diffusion equation has also previously been used to treat light emission and lasers in compound semiconductors.[14,15] We, therefore, adopt a drift-diffusion treatment for carrier transport and light emission in the long-CNT channel. The electrons (holes) satisfy the continuity equation in the channel,[13]

$$\frac{dn}{dt} = \frac{1}{q}\frac{dJ_n}{dx} - R, \quad \frac{dp}{dt} = -\frac{1}{q}\frac{dJ_p}{dx} - R, \tag{2}$$

where $dn/dt = dp/dt = 0$ at the steady state, and J_n (J_p) is the electron (hole) current computed by drift-diffusion equation. (The mobility in semiconducting CNTs is characterized to be 1000–100 000 cm^2/V s at low field,[11,12,16] and it decreases at high field.[17] A mobility value of $\mu = 1000$ cm^2/V s is used in this study, and the role of mobility will be further discussed later.) R is the radiative band-to-band recombination rate (the photon emission rate),[13]

$$R = B(np - n_i^2), \tag{3}$$

where $n(p)$ is the electron (hole) density, n_i is the intrinsic carrier density, and B is the bimolecular recombination coefficient that is determined by the strength of radiative recombination in the material. Notice that the measured size of the light spot (2–4 μm),[7] which is controlled by B and μ, is an indication of recombination strength. A larger B (which corresponds to a shorter recombination lifetime) or a smaller μ (which corresponds to a slower carrier velocity) results in a smaller size of the light spot. By fitting to the experimentally measured size of the light spot, a value of $B \approx 200$ cm/s is obtained for $\mu = 1000$ cm^2/V s. For determining an accurate value of B, accurate characterization for the size of the light spot and the carrier mobility is needed.

The semiclassical treatment of the channel is coupled to the quantum treatment of the contacts in the following way. Because the length scale over which tunneling occurs is much shorter than the total channel length, the current computed by Eq. (1) is imposed as a current boundary condition to the drift-diffusion equation in the channel.[18,19] Carrier injection into the gate oxide is not treated.

We first investigate the role of self-consistency between electrostatics and carrier transport. Figure 2(a) plots the conduction and valence bands versus the channel position at $V_G = V_D/2 = -1.01$ V. Because the channel length is much larger than the gate oxide thickness, most of the channel is well controlled by the gate, and the Laplace solution, which omits the charge in the channel, remains flat along the channel. In order to sustain the hole (electron) tunneling current injected from the source (drain) contact, a diffusion current is needed in the channel. As a result, the hole (electron) density reaches its peak value near the source (drain), and linearly drops toward the drain (source). The net charge density is positive near the source, but negative near the drain. A self-consistent potential with an electric field along the channel is produced by this charge distribution, as shown by the solid lines in Fig. 2(a), and drives a drift current in the channel. In ambipolar transport regime, self-consistency between electrostatics and transport results in opposite charge density peaks at the two ends of the channel, which provide the driving force for both drift and diffusion currents through the channel.

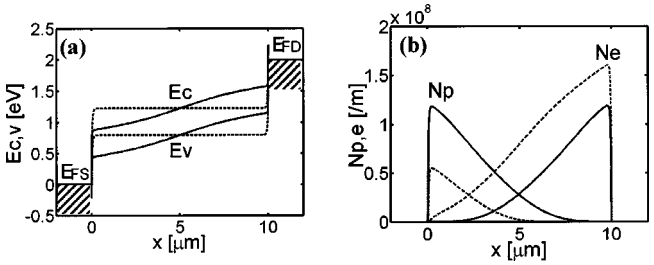

FIG. 2. Band profile and charge density in a CNTFET with a channel length $L_{ch} = 10$ μm. (a) The conduction and valence bands vs the channel position at $V_G = -1.01$ V and $V_D = -2.02$ V. The solid lines are the self-consistent solution, and the dashed lines are the Laplace solution (which omits charge in the channel). (b) Hole density (with a peak value near the source) and electron density (with a peak value near the drain) vs the channel position for two bias conditions. The solid lines are for $V_G = -1.01$ V, $V_D = -2.02$ V, and the dashed lines are for $V_G = -0.95$ V, $V_D = -1.99$ V.

Next, we explore how infrared emission affects carrier transport in the channel. The curves (i) in Fig. 3(a) plot the hole and electron current versus the channel position for a long-channel CNTFET ($L_{ch} = 10$ μm) exactly biased at ambipolar condition.[9,20] The electron current I_e injected from the drain equals to the hole current, I_h, injected from the source. The radiative recombination rate, $R = B(np - n_i^2)$, reaches its maximum value at the middle of the channel, where the electron density, n, is close to the hole density, p. Both the electron current and the hole current are strongly position-dependent near the light-emission spot at the middle of the channel. When the channel length is longer than the radiative recombination length, electrons and holes are completely annihilated in the channel, and the total source–drain current, $I_D = I_e = I_h \approx -0.10$ μA. For comparison, we also simulated a CNTFET with a channel length ($L_{ch} = 1$ μm) shorter than the radiative recombination length ((2–4 μm[7]). In contrast, the effect of radiative process on carrier transport

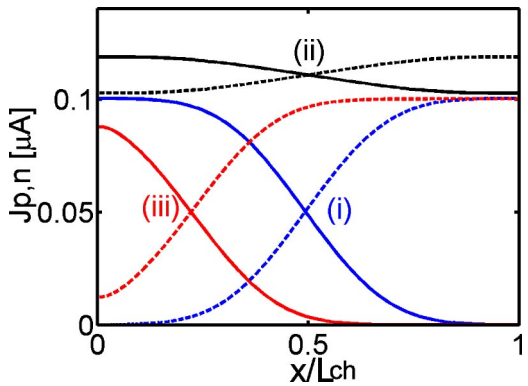

FIG. 3. (Color online) Hole current injected from the source (solid) and electron current injected from the drain (dashed) vs the normalized channel position for (i) $L_{ch} = 10$ μm, $V_G = -1.01$ V, $V_D = -2.02$ V, (ii) shorter channel with $L_{ch} = 1$ μm, $V_G = -1.01$ V, $V_D = -2.02$ V, and (iii) $L_{ch} = 10$ μm, $V_G = -0.95$ V, $V_D = -1.99$ V.

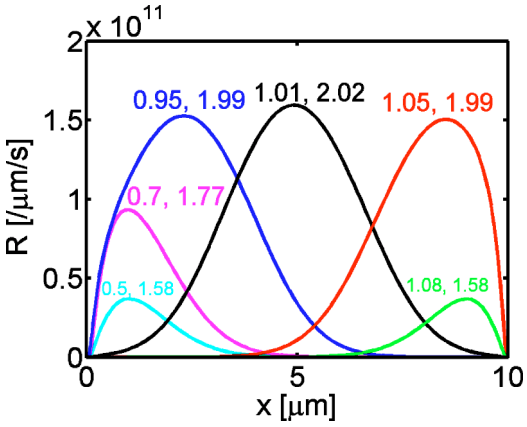

FIG. 4. (Color online) Radiative recombination rate (photon emission rate) vs channel position when V_G and V_D sweep. The source–drain current is kept constant at $I_D \approx -0.10$ μA throughout the bias sweep. The numbers labeled near the peak of each curve are $(-V_G, -V_D)$ in units of volts.

is much weaker. As shown by curves (ii) in Fig. 3, both the electron and hole currents are nearly position-independent throughout the channel. The total source–drain current, $I_D \approx -0.20$ μA, is two times larger than the value for the long-channel CNTFET. Because the channel length is shorter than the recombination length, a significant portion of holes (electrons) injected from the source (drain) flow out of the drain (source), and the complete carrier annihilation in the channel does not occur. How significantly radiative process affects carrier transport in the channel depends on how the channel length compares with the radiative-recombination length. For a stronger recombination process, radiative process starts to play an important role at a shorter channel length.

As shown by curves (i) in Fig. 3, the current at the source end of the channel is completely due to holes and the current at the drain end completely due to electrons for a long-CNTFET exactly biased at the ambipolar condition. Complete separation of the electron and hole currents,[7] however, only occurs when the CNTFET is exactly biased at the ambipolar condition, and the radiation peak is at the middle point of the channel. Even for a bias condition slightly deviated, the complete separation does not occur. As shown by the curves (iii) in Fig. 3, which plots the electron current and the hole current versus the channel position at $V_G = -0.95$ V and $V_D = -1.99$ V, the hole injection from the source is lower than the electron injection from the drain, which is not sufficient to completely annihilate the electrons injected from the drain. As a result, the electron current near the source end of the channel is nonzero. The current near the drain is completely supplied by electrons, but the current near the source is by both electrons and holes.

We finally explore the light-spot movement along the CNT channel, an interesting behavior of CNT IR emitters.[7] Figure 4 plots the radiative recombination rate versus the channel position for different bias points in a voltage sweep. The source–drain current is kept constant at about -0.10 μA throughout the voltage sweep. At the exact ambipolar bias point ($V_G = V_D/2 = -1.01$ V), the hole injection from the source equals to the electron injection from the drain, and the radiative peak appears exactly at the middle of the channel. For $|V_G| < |V_D|/2$, the hole density decreases and the electron density in the channel increases. [For example, see the dashed lines in Fig. 2(b), which plots the electron and hole densities at $V_G = -0.95$ V and $V_D = -1.99$ V.] The position where $n = p$ shifts toward the source, and the light spot moves toward the source. Similarly, for $|V_G| > |V_D|/2$, the electron density reduces and the hole density increases, and the light spot moves toward the drain.

The following features are observed in the simulation. When the gate voltage varies from 0 to -0.95 V, the light emission spot stays near the source, and the intensity increases when the magnitude of V_G increases. The light spot only starts to move when V_G is very close to the exact ambipolar bias, $V_G = -1.01$ V. As V_G varies from -0.95 to -1.05 V, the light spot rapidly moves from the source end to the drain end of the channel, and the peak value of light emission remains nearly constant. As V_G further varies from -1.05 to -1.09 V, the light spot stays near the drain, and the intensity decreases. Compared to the experiment, the simulation results capture the major features of the light-spot movement.[7] The agreement indicates that the movement of the light spot can be mostly understood by a simple, semiclassical picture.

The authors thank Professor Mark Lundstrom of Purdue University and Dr. Phaedon Avouris of IBM T. J. Watson Research Center for extensive technical discussions. This work was supported by the start-up fund for J.G. at University of Florida, and the NSF Network for Computational Nanotechnology. The computational facility was made possible from the NSF Grant No. EIA-0224442, IBM SUR grants and gifts, and a DURIP Grant from Army Research Office.

[1] P. L. McEuen, M. S. Fuhrer, and H. K. Park, IEEE Trans. Nanotechnol. **1**, 78 (2002).
[2] P. Avouris, J. Appenzeller, R. Martel, and S. Wind, Proc. IEEE **91**, 1772 (2003).
[3] J. A. Misewich, R. Martel, Ph. Avouris, J. C. Tsang, S. Heinze, and J. Tersoff, Science **300**, 783 (2003).
[4] M. Freitag, Y. Martin, J. A. Misewich, R. Martel, and Ph. Avouris, Nano Lett. **3**, 1067 (2003).
[5] M. S. Arnold, J. E. Sharping, S. I. Stupp, P. Kumar, and M. Hersam, Nano Lett. **3**, 1549 (2003).
[6] Z. Wu, Z. Chen, X. Du, J. M. Logan, J. Sippel, M. Nikolou, K. Kamaras, J. R. Reynolds, D. B. Tanner, A. R. Hebard, and A. G. Rinzler, Science **305**, 1273 (2004).
[7] M. Freitag, J. Chen, J. Tersoff, J. C. Tsang, Q. Fu, J. Liu, and Ph. Avouris, Phys. Rev. Lett. **93**, 076803 (2004).
[8] Notice that the spectrum peak of emitted light appears near a wavelength determined by the nantoube band gap (diameter), $\lambda_{peak} \sim 1.5$ μm$\times d$ (in nanometers), and the experiment in Ref. 1 measured at $\lambda \sim 2$ μm for a 3-nm-diam tube, which is the high energy tail of the emitted light.
[9] J. Guo, S. Datta, and M. Lundstrom, IEEE Trans. Electron Devices **51**, 172 (2004).
[10] S. Datta, *Electronic Transport in Mesoscopic Systems* (Cambridge University Press, New York, 1995).
[11] A. Javey, J. Guo, Q. Wang, M. Lundstrom, and H. J. Dai, Nature (London) **424**, 654 (2003).
[12] S. Rosenblatt, Y. Yaish, J. Park, J. Gore, V. Sazonova, and P. L. McEuen, Nano Lett. **2**, 869 (2002).
[13] S. M. Sze, *Physics of Semiconductor Devices* (Wiley, New York, 1981).
[14] A. A. Grinberg, M. A. Alam, and S. K. Sputz, IEEE J. Quantum Electron. **35**, 84 (1999).
[15] M. Alam, M. Hybertsen, R. Smith, and G. Baraff, IEEE Trans. Electron Devices **47**, 1917 (2000).
[16] T. Durkop, S. Getty, E. Cobs, and M. Fuhrer, Nano Lett. **4**, 35 (2004).
[17] G. Pennington and N. Goldsman, Phys. Rev. B **68**, 045426 (2003).
[18] C. K. Huang, W. E. Zhang, and C. H. Yang, IEEE Trans. Electron Devices **45**, 842 (1998).
[19] M. Ieong, P. Solomon, S. Laux, H. S. P. Wong, and D. Chidambarrao, Tech. Dig. - Int. Electron Devices Meet. **1998**, 733.
[20] M. Radosavljevic, S. Heinze, J. Tersoff, and Ph. Avouris, Appl. Phys. Lett. **83**, 2435 (2003).